6432 J. Med. Chem. 2010, 53, 6432–6444
DOI: 10.1021/jm100498u

Journal of Medicinal Chemistry Article

p-Trifluoromethyldiazirinyl-etomidate: A Potent Photoreactive General Anesthetic Derivative of Etomidate That Is Selective for Ligand-Gated Cationic Ion Channels

S. Shaukat Husain,[‡] Deirdre Stewart,[‡] Rooma Desai,[‡] Ayman K. Hamouda,[§] S. Guo-Dong Li,[∥] Elizabeth Kelly,[‡] Zuzana Dostalova,[‡] Xiaojuan Zhou,[‡] Joseph F. Cotten,[‡] Douglas E. Raines,[‡] Richard W. Olsen,[∥] Jonathan B. Cohen,[§] Stuart A. Forman,[‡] and Keith W. Miller*[,‡,#]

[‡]*Department of Anesthesia, Critical Care and Pain Medicine, Massachusetts General Hospital, 32 Fruit Street, Boston, Massachusetts 02114,* [#]*Department of Biological Chemistry and Molecular Pharmacology , and* [§]*Department of Neurobiology, 220 Longwood Avenue, Harvard Medical School, Boston, Massachusetts 02115, and* [∥] *Department of Molecular and Medical Pharmacology, Geffen School of Medicine, University of California at Los Angeles, Los Angeles, California 90095*

Received April 22, 2010

We synthesized the R- and S-enantiomers of ethyl 1-(1-(4-(3-((trifluoromethyl)-3*H*-diazirin-3-yl)-phenyl)ethyl)-1*H*-imidazole-5-carboxylate (trifluoromethyldiazirinyl-etomidate), or TFD-etomidate, a novel photoactivable derivative of the stereoselective general anesthetic etomidate (*R*-(2-ethyl 1-(phenylethyl)-1*H*-imidazole-5-carboxylate)). Anesthetic potency was similar to etomidate's, but stereoselectivity was reversed and attenuated. Relative to etomidate, TFD-etomidate was a more potent inhibitor of the excitatory receptors, nAChR (nicotinic acetylcholine receptor) ($(\alpha1)_2\beta1\delta1\gamma1$) and 5-$HT_{3A}$R (serotonin type 3A receptor), causing significant inhibition at anesthetic concentrations. *S*- but not *R*-TFD-etomidate enhanced currents elicited from inhibitory $\alpha1\beta2\gamma2$L $GABA_A$Rs by low concentrations of GABA, but with a lower efficacy than *R*-etomidate, and site-directed mutagenesis suggests they act at different sites. [^{3}H]TFD-etomidate photolabeled the α-subunit of the nAChR in a manner allosterically regulated by agonists and noncompetitive inhibitors. TFD-etomidate's novel pharmacology is unlike that of etomidate derivatives with photoactivable groups in the ester position, which behave like etomidate, suggesting that it will further enhance our understanding of anesthetic mechanisms.

Introduction

Etomidate (*R*-2-ethyl 1-(phenylethyl)-1*H*-imidazole-5-carboxylate) is one of the most potent general anesthetic drugs in clinical use. It causes anesthesia with a half effective concentration of ~2 μM.[1,2] Etomidate interacts with members of the Cys-loop ligand-gated ion channel superfamily of receptors, which include subtypes activated by γ-amino butyric acid (GABA),[a] glycine, serotonin (5-HT), and acetylcholine (ACh). $GABA_A$R is the most sensitive to etomidate,[3−6] which acts as a positive allosteric mediator, enhancing GABA-induced currents by increasing the receptor's open state probability, resulting in a shift in the agonist concentration−response curve to lower concentrations.[7,8] At higher concentrations, etomidate can activate $GABA_A$Rs directly and also acts as a negative allosteric inhibitor on the cationic ligand-gated excitatory receptors, 5-HT_{3A}R and nAChR.[5,6]

Because of the above selectivity, which it shares with another high affinity anesthetic, propofol,[7] more progress has been made in understanding the mechanism of etomidate's action than for most other general anesthetics. In $\alpha1\beta1\gamma2$L $GABA_A$Rs, a residue on the β-subunit 15 residues from the conserved charge at the cytoplasmic end of the channel (M2 15′ N265) is a determinant of sensitivity to etomidate.[3,9,10] It is located contralateral to the ion channel, facing the interior of the subunit's four transmembrane helix bundle, a region that is hypothesized to be a binding pocket for inhalation anesthetics on other subunits.[11] Mutations at this position in knock-in mice can ablate etomidate's and propofol's anesthetic action, while having little effect on that of inhalation anesthetics.[12−14] However, this residue is not part of an anesthetic binding pocket because it changes etomidate's efficacy much more than its affinity,[15] and propofol is unable to protect cysteines substituted at this position from chemical modification.[16]

A definitive way to locate etomidate's binding site(s) is to use derivatives of etomidate that are photoactivable. One such agent, azietomidate or [2-(3-methyl-3Hdiaziren-3-yl)ethyl

*Corresponding author. Phone: (617) 726-8985. Fax: (617) 724-8644. E-mail: k_miller@helix.mgh.harvard.edu.

[a] Abbreviations: 5-HT, serotonin; 5-HT_{3A}R, 5-HT receptor, subtype 3A; ACh, acetylcholine; azietomidate, *R*-2-(3-methyl-3*H*-diaziren-3-yl)-ethyl 1-(1-phenylethyl)-1*H*-imidazole-5-carboxylate; BzBzl-etomidate, *R*-4-benzoylbenzyl-1-(1-phenylethyl)-1*H*-imidazole-5-carboxylate; DBU, 1,8-diazabicyclo[5.4.0]-undec-7-ene; EC_{50}, concentration required for 50% of full effect; [^{3}H]EBOB, [^{3}H]ethynylpropylbicycloorthobenzoate; etomidate, *R*-2-ethyl 1-(phenylethyl)-1*H*-imidazole-5-carboxylate; LORR, loss of righting reflexes; GABA, γ-amino butyric acid; $GABA_A$R, Type A GABA receptor chloride channel; IC_{50}, concentration required for 50% of full inhibitory effect; n_H = Hill coefficient; nAChR, nicotinic acetylcholine receptor ion channel; octanol, octan-1-ol; SD, standard deviation; TDBzl-etomidate, *R*-4-[3-(trifluoromethyl])-3*H*-diazirin-3-yl]-benzyl 1-(1-phenylethyl)-1*H*-imidazole-5-carboxylate; TFD-etomidate, *p*-trifluoromethyldiazirinyl-etomidate or ethyl 1-(1-(4-(trifluoromethyl)-3*H*-diazirin-3-yl)phenylethyl)-1*H*-imidazole-5-carboxylate; THF, tetrahydrofuran; TFA, trifluoroacetic acid; VDAC, voltage-dependent anion channel.

 Published on Web 08/12/2010

Scheme 1. Photoactivable Derivatives of the General Anesthetic Etomidate

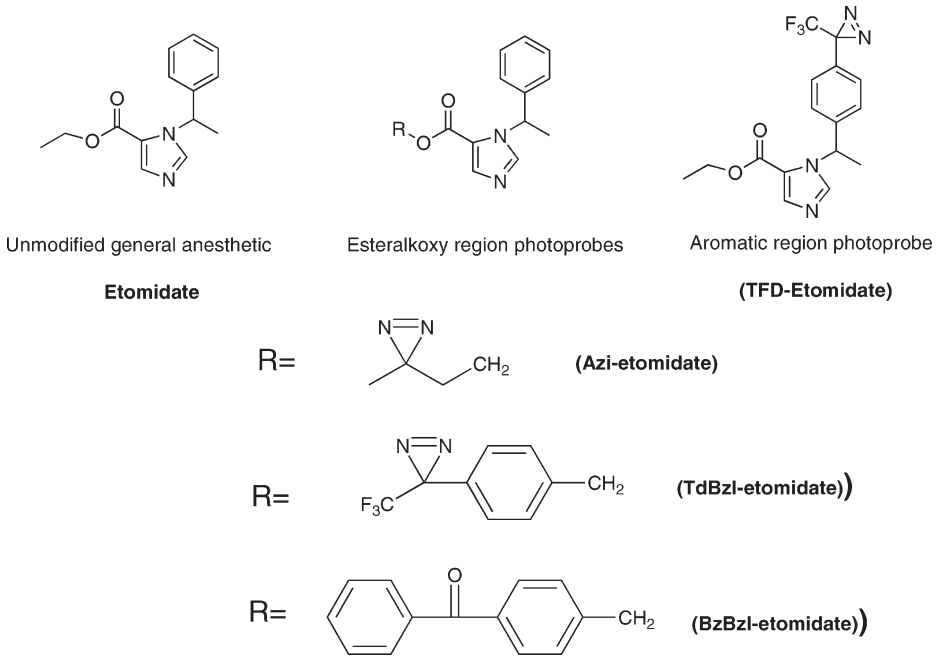

1-(1-phenylethyl)-1*H*-imidazole-5-carboxylate], in which an ethoxy group has been replaced by a 3-azibutoxy group, exhibits potency and pharmacology very similar to the parent compound in $GABA_A$Rs, tadpoles and rodents.[5] Furthermore, in etomidate-resistant knock-in mice bearing a N265M mutation in the β3-subunit of the $GABA_A$ receptor, azietomidate's potency is attenuated in parallel with that of etomidate.[17] Azietomidate photolabels $GABA_A$Rs from bovine cortex in an agonist-dependent manner, and two residues, which appeared from pharmacological analysis to be part of a single binding pocket, were identified, one on the αM1 and the other on the βM3 transmembrane helix. Homology modeling suggests that these residues are located not within the intra-subunit four helix bundle but in the interface between the α- and β-subunits.[18]

To further test the subunit interface site hypothesis, we adopted the long-term goal of devising a set of two etomidate derivatives that have photoactivable moieties on opposite ends of the molecule. We have to date investigated the pharmacology of two more ester substituents. Both benzophenone- and aryl diazirine-derivatives of etomidate (Scheme 1) proved to be potent general anesthetics that modulate $GABA_A$R function.[5,6]

In this manuscript, we describe the synthesis and initial pharmacologic characterization of ethyl 1-(1-(4-(trifluoromethyl)-3*H*-diazirin-3-yl)phenylethyl)-1*H*-imidazole-5-carboxylate (trifluoromethyldiazirinyl-etomidate), or TFD-etomidate (Schemes 1 and 2). In this derivative, the TFD moiety modifies etomidate's benzyl group and is thus complementary to TDBzl-etomidate, in which the same moiety is substituted at etomidate's ethoxy group. We determined that TFD-etomidate, like etomidate, is a potent general anesthetic that interacts with and modulates the $GABA_A$R, *Torpedo* nAChR, and 5-HT_{3A}R. However, we found it has a unique selectivity for cation conducting Cys-loop receptors relative both to etomidate and to the other previously developed etomidate photolabel derivatives.

Chemistry

The synthesis of TFD-etomidate is outlined in Scheme 2. The key intermediate for the preparation of the photoactivatable etomidate analogue was the protected diazirine, 3-(4-(1-(*tert*-butyl)dimethylsilyloxy)ethyl)phenyl)-3-((trifluoromethyl)-3H-diazirine (**7**). Its synthesis involved protection of the hydroxyl group of the starting compound 4-bromo-α-methylbenzyl alcohol (**1**) with the acid labile tert-butyldimethyl silyl group, conversion of the bromo group of the protected derivative to trifluoromethylketone (**3**), and subsequent conversion of the keto group via a series of reactions to the diazirinyl functional group. Synthesis of TFD-etomidate from the silyl-protected diazirine (**7**) was performed by two alternate routes: Using the first route, the silyl protecting group was replaced by the bromo group, which after reaction with ammonia gave the aryl amine (**9**). TFD-etomidate was synthesized from the aryl amine utilizing the route originally developed by Godefroi et al.[1] for the synthesis of etomidate. Since the synthetic sequence involved reaction at the chiral center during conversion of the bromo compound to the amine, the final product was a racemate. The racemic mixture of TFD-etomidate was resolved by chromatography on Chiracel OD-H column. After the above synthesis of TFD-etomidate was completed, Zolle et al[19] described conditions for Mitsunobu coupling between chiral precursor alcohols with methyl 1*H*-imidazole-5-carboxylate. This reaction yielded enantiomerically pure analogues of etomidate having a reversed chirality compared to that of the starting alcohol. Following these conditions and starting with *R*- or *S*- diazirinyl alcohols (**14**), produced by reaction of the silyl-protected diazirine derivative (**7**) that we had already synthesized, application of the Mitsunobu reaction provided R- and S- enantiomers of TFD-etomidate.

Results

Solubility and Partition Coefficient. The saturated solubility of TFD-etomidate when thoroughly equilibrated in 0.01 M Tris-HCl buffer, pH 7.4, was 58 μM. It should be noted that higher concentrations were easily achieved in fresh solutions with crystalline solid only precipitating the next day. Thus, in some physiological experiments herein freshly made supersaturated solutions were used.

Scheme 2. Synthesis of TFD-etomidate[a]

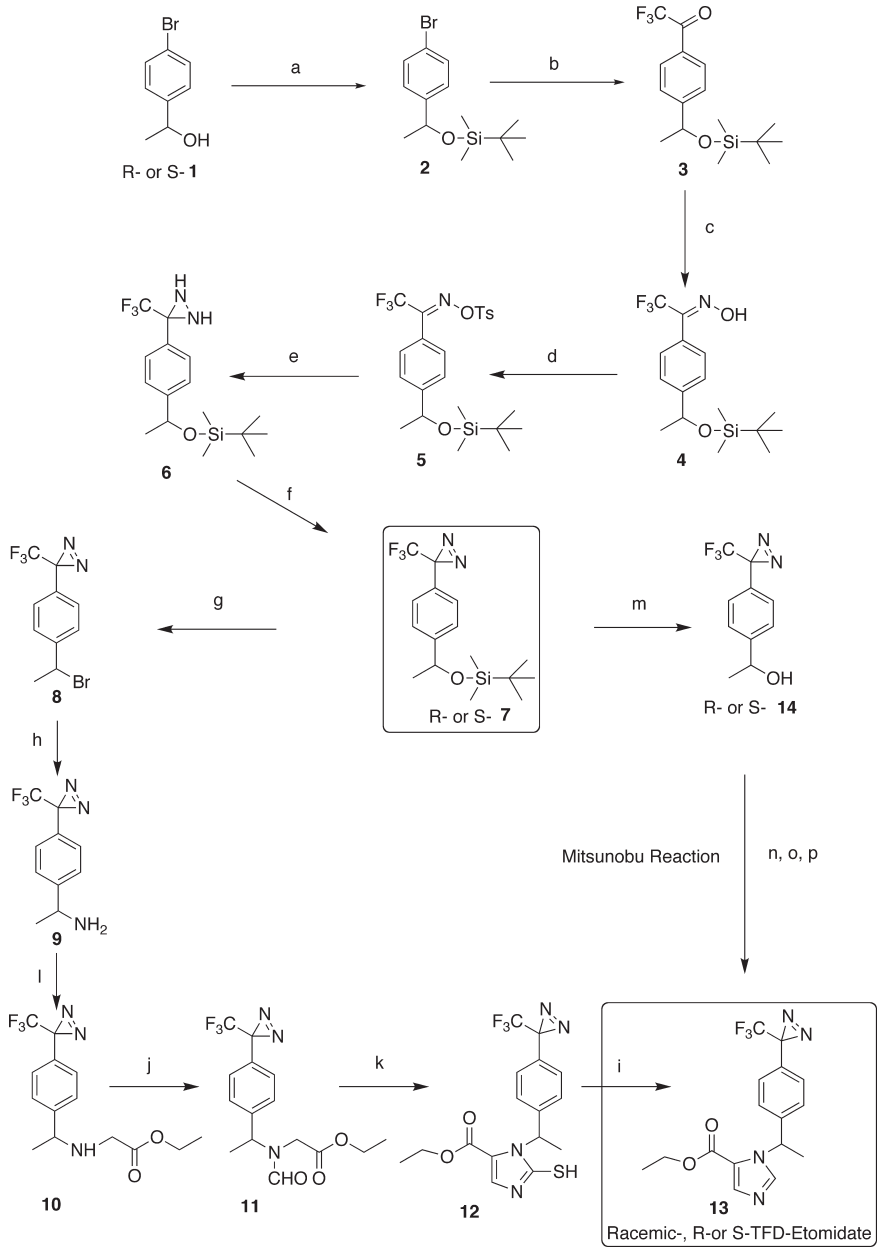

[a] (a) *tert*-Butyldimethylsilyl chloride, DBU, dichloromethane; (b) (i) *n*-butyllithium, THF, (ii) diethyl trifluoroacetamide, THF; (iii) water/ammonium chloride; (c) hydroxylamine hydrochloride, pyridine; (d) *p*-toluene sulfonyl chloride, triethylamine, dimethylamino pyridine, dichloromethane; (e) liquid ammonia, ether; (f) iodine, triethylamine, dichloromethane; (g) triphenylphosphine dibromide, dichloromethane; (h) ammonia, methanol; (i) ethyl chloroacetate, triethylamine, DMF; (j) formic acid, diisopropyl carbodiimide, pyridine, dichloromethane; (k) (i) paraffinic sodium suspension, THF, ethanol, ethyl formate, (ii) conc. HCl, KSCN, water; (l) sodium nitrite, nitric acid, water, chloroform; (m) (i) tetrabutylammonium fluoride, THF, (ii) ammonium chloride. Mitsunobu reaction: (n) ethyl 1*H*-imidazole-5-carboxylate, THF; (o) triphenylphosphine, THF; (p) *tert*-butylazodicarboxylate, THF.

The octanol/Tris buffer partition coefficient of TFD-etomidate was 27 000. In comparison, we found the partition coefficient for etomidate to be 330 under the same conditions. This compares to a previously reported value, determined in unbuffered water, of 776.[20] Thus, substitution of etomidate's aromatic ring with a trifluoromethyldiazirinyl group results in an increase in the partition coefficient by almost 2 orders of magnitude. The partition coefficient for TFD-etomidate is comparable to those for TDBzl-etomidate and BzBzl-etomidate, which have values of 19 000 and 25 000, respectively.[6] Enantioselectivity is not expected in physical properties, and because of the limited quantities of the enantiomers, their solubility was not examined.

General Anesthetic Potency. With institutional approval, the general anesthetic potency of TFD-etomidate was assayed in tadpoles. TFD-etomidate induced a reversible general anesthetic state that resembled that of etomidate. Tadpoles that had lost their righting reflexes showed a brief response to a light touch and even twitched spontaneously, behaviors that differ from conventional general anesthetics. The onset of and recovery from anesthesia was somewhat

slower than for etomidate, with the fraction anesthetized becoming constant after 30−40 min; however, the potency of the two agents was comparable. The concentration-dependence of LoRR was examined in groups of five animals at seven concentrations between 0.25 and 25 μM. The EC_{50} and number of animals for *S*- and *R*-TFD-etomidate was 4.9 ± 0.15 μM (45 animals; all errors herein are standard deviations unless otherwise stated) and 17.1 ± 0.35 μM (47 animals) respectively, comparable to two prior studies with *R*- and *S*-etomidate that gave EC_{50}'s of 2.3 ± 0.13 and 25 ± 2.2 μM, respectively.[2,5] Only animals that fully recovered in fresh water overnight were included in the analysis. At 20 μM, 2 of 5 animals died but none of 10 at 22.5 and 25 μM.

Action on $GABA_A$ Receptor Physiology. In human $\alpha1\beta2\gamma$-2L $GABA_A$Rs expressed in *Xenopus* oocytes at low (10 μM) and maximal (0.1−10 mM) concentrations of GABA, racemic TFD-etomidate (5 μM) elicited much smaller enhancements of currents than etomidate at the same concentration. GABA concentration response curves (± drugs) were determined at fixed concentration of anesthetic equal to twice the EC_{50} for tadpole anesthesia, a concentration generally considered to represent clinical anesthesia. The GABA concentration−response curve was shifted to the left 1.8-fold by 5 μM TFD-etomidate but 18-fold by the same concentration of *R*-etomidate (data not shown). Similar experiments were done with the R- and S-enantiomers of TFD-etomidate. At twice the tadpole EC_{50}, *S*-TFD-etomidate (10 μM) shifted the GABA concentration response curve to the left 2.6-fold without a change in the maximum current (Figure 1A), whereas *R*-TFD-etomidate (34 μM) shifted the GABA concentration response curve 1.2-fold to the right and decreased the maximum current (Figure 1B). At 10 μM GABA, 10−100 μM *R*-TFD-etomidate inhibited the response up to 20%.

These observations suggested that TFD-etomidate and etomidate might have different sites of action. To test this hypothesis, we employed the mutant GABA receptor $\alpha1\beta2M286W\gamma2L$ that lacks etomidate sensitivity.[21] For wild type ($\alpha1\beta2\gamma2L$) GABA receptors, in the same oocyte 3 μM GABA currents were increased 2.2- and 3.0-fold by 5 and 10 μM *S*-TFD-etomidate, respectively, compared to an increase of 3.7-fold with 5 μM *R*-etomidate (Figure 1C, top line of traces). Using the mutant GABA receptor in a similar experiment, the action of 5 and 10 μM *S*-TFD was similar to that of the wild type receptor, a 1.8- and 2.2-fold increase respectively in 1 μM GABA currents (1 and 3 μM GABA elicit a current one-tenth of I_{max}, that is, EC_{10}, in mutant and wild type receptors, respectively), whereas 5 μM etomidate caused no change (Figure 1C, bottom line of traces). Furthermore, TFD-etomidate (0−30 μM) caused a linear increase in 3 μM GABA currents in wild type receptors of up to 2.5-fold that was not attenuated by the presence of 1 μM etomidate (the slope was 0.05 ± 0.001 in each case). These results are consistent with the separate site hypothesis.

TFD-etomidate, like etomidate,[5] could directly activate currents in the absence of GABA (data not shown), but once again its action was weaker than etomidate's. Saturated concentrations of TFD-etomidate induced a current that was 1.3% of that elicited by 10 mM GABA, whereas the comparable figure for 30 μM etomidate was 27%. The effect with TFD-etomidate was too small to make it worth addressing the question of enantioselectivity.

Allosteric Modulation of $GABA_A$ Receptor. To compare their allosteric action, the effects of various concentrations of etomidate and TFD-etomidate on 1 nM [^{3}H]flunitrazepam or

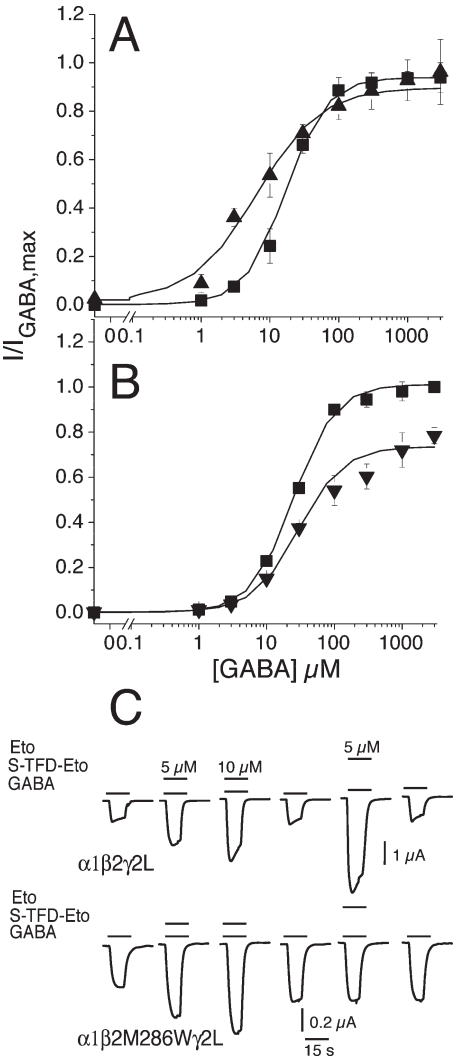

Figure 1. Etomidate and TFD-etomidate modulation of GABA-induced currents through human wild type $\alpha1\beta2\gamma2L$ $GABA_A$ receptors expressed in *Xenopus* oocytes. GABA concentration response curves were measured before and after the addition of drug, with 2−3 recordings done at each concentration. Current recordings were normalized to the maximal GABA response. (A) Data shown for the experiment with *S*-TFD-etomidate represent experiments on three different oocytes. Nonlinear least-squares fitting gave (EC50 in μM and Hill coefficient, n_H): for the GABA control (■), EC_{50} = 17 ± 2, n_H = 1.5 ± 0.1, I_{max} = 0.9 ± 0.02, and in the presence of 10 μM *S*-TFD-etomidate (▲), EC_{50} = 6.4 ± 1.6, n_H = 0.9 ± 0.2, I_{max} = 0.90 ± 0.05. (B) The experiment with *R*-TFD-etomidate was done on one oocyte due to the high concentration of reagent needed. For the GABA control (■), EC_{50} = 25 ± 1, n_H = 1.4 ± 0.1, I_{max} = 1.01 ± 0.01. In the presence of 34 μM *R*-TFD-etomidate (▼), EC_{50} = 30 ± 2.5, n_H = 1.3 ± 0.04, I_{max} = 0.73 ± 0.02. (C) *S*-TFD-etomidate modulates an etomidate-insensitive mutant. The top line of current traces show the effects of the applications of *S*-TFD-etomidate and *R*-etomidate on 3 μM GABA currents elicited from wild type ($\alpha1\beta2\gamma2L$) $GABA_A$ receptors using 5 and 10 μM *S*-TFD-etomidate and then 5 μM *R*-etomidate. The bottom line of current traces shows the same series of applications of drugs on 1 μM GABA currents elicited from the mutant ($\alpha1\beta2M286W\gamma2L$) GABA receptor.

5 nM [^{3}H]muscimol binding to cerebral cortex membranes were examined (Figure 2). Etomidate enhanced [^{3}H]flunitrazepam binding at concentrations up to 10 μM with a subsequent decrease (Figure 2A). The enhancement of binding was detectable at 0.1 μM etomidate and reached a plateau at ~10 μM with

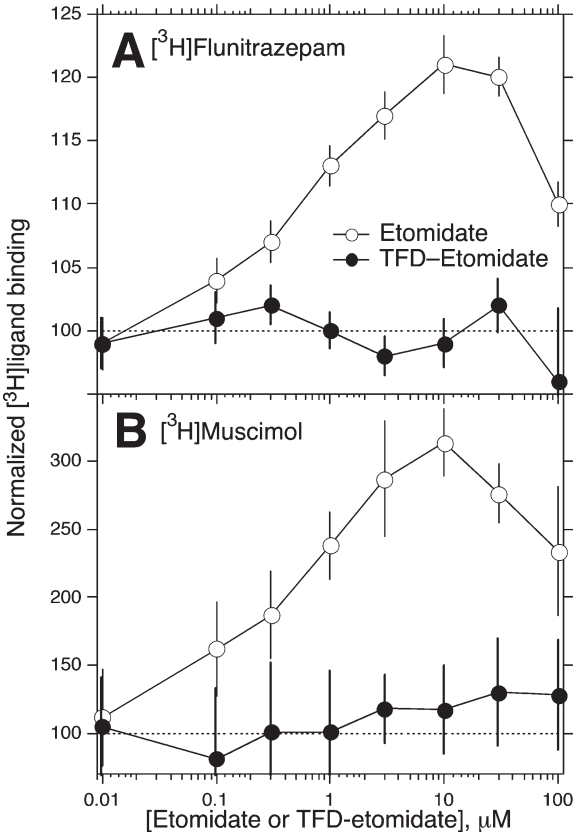

Figure 2. TFD-etomidate does not interact allosterically with GABA$_A$ receptor ligands. Effect of TFD-etomidate and etomidate on (A) 1 nM [^{3}H]flunitrazepam binding; (B) 5 nM [^{3}H]muscimol binding both to cerebral cortex membranes.

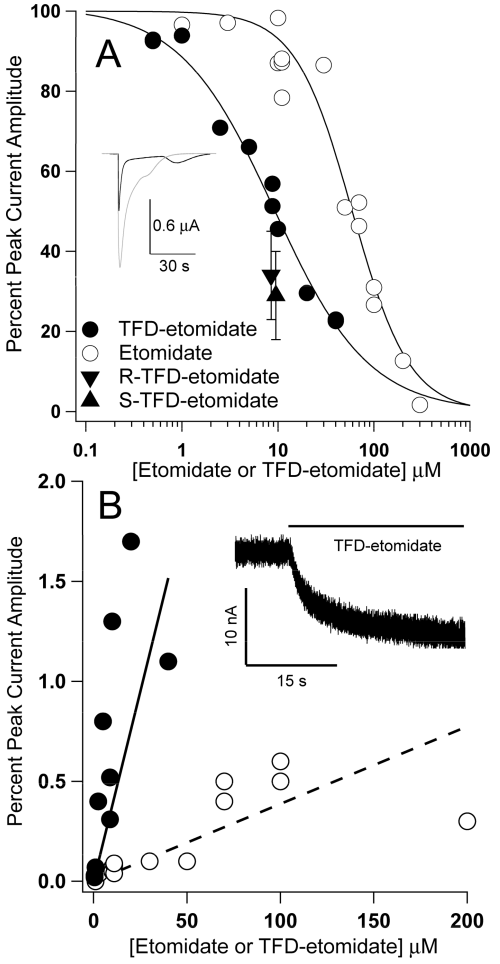

Figure 3. Actions on the 5-HT$_{3A}$ receptor of TFD-etomidate and etomidate. (A) Anesthetic concentration-dependence of the percent peak current amplitude evoked by 100 μM 5-HT. For both agents, the percent peak current amplitude decreased with anesthetic concentration. The IC$_{50}$'s were $60 \pm 5\,\mu$M and $9 \pm 1\,\mu$M and $n_H = 1.5 \pm 0.2$ and 0.9 ± 0.1 for etomidate and TFD-etomidate, respectively. The inset shows representative current traces (100 μM 5-HT) obtained in the absence of anesthetic (gray) and in the presence of 10 μM TFD-etomidate. (B) Anesthetic concentration-dependence for currents activated in the absence of agonist. The ordinate is normalized to the current elicited by 100 μM 5-HT. For both etomidate and TFD-etomidate, this activation current increased linearly with anesthetic concentration with slopes of $3.9 \pm 0.4\,\mu M^{-1}$ and $38 \pm 0.8\,\mu M^{-1}$ for etomidate and TFD-etomidate, respectively. The inset shows a representative current trace obtained upon application of 10 μM TFD-etomidate alone.

a ~1.2-fold maximal enhancement of [^{3}H]flunitrazepam binding. The concentration dependence of etomidate enhancement could be fit to a logistic curve, yielding half-effect concentrations of $0.94 \pm 0.45\,\mu$M. In contrast, TFD-etomidate failed to show modulation of [^{3}H]flunitrazepam binding: it caused neither enhancement nor inhibition in the concentration range tested (Figure 2A).

Etomidate caused ~3-fold maximal enhancement of [^{3}H]muscimol binding at a concentration of 10 μM and a subsequent decrease at higher concentrations (Figure 2B). The concentration dependence of enhancement could be fit to a logistic curve, yielding a half-effect concentration of $0.42 \pm 0.21\,\mu$M. In comparison, TFD-etomidate failed to show any modulation of [^{3}H]muscimol binding. There was no enhancement or inhibition in the concentration range tested (Figure 2B).

Inhibition of 5-HT$_{3A}$ Receptor by TFD-etomidate. Figure 3 shows that in oocytes expressing 5-HT$_{3A}$Rs, both racemic TFD-etomidate and *R*-etomidate inhibited currents evoked by 100 μM 5-HT. The magnitude of this inhibition increased with anesthetic concentration and upon simultaneous termination of anesthetic and agonist, a surge current was recorded (inset). Although the inhibitory actions of TFD-etomidate and etomidate were qualitatively similar, TFD-etomidate inhibited currents with an IC$_{50}$ that was 7-fold lower than etomidate and with a Hill coefficient of -1 rather than -2 for etomidate (see legend to Figure 3). At a fixed concentration of 9 μM, *S*- and *R*-TFD-etomidate caused equal inhibition of 29 ± 11 (n = 9) and $34 \pm 11\%$ (n = 13) of control, respectively, compared to the racemic compound $28 \pm 11\%$ (n = 4) in a parallel experiment. The action of etomidate was also without marked stereoselectivity (not shown).

In addition to inhibiting currents, both TFD-etomidate and *R*-etomidate evoked a small current prior to the application of 5-HT as shown on the inset in Figure 3B. The peak amplitudes of such directly activated currents are plotted as a percentage of the current evoked by 100 μM 5-HT versus anesthetic concentration. In general, the amplitude of this directly activated current increased with anesthetic concentration, reaching 1.7% and 1.3% of that evoked by 100 μM 5-HT at 20 μM TFD-etomidate and 300 μM etomidate, respectively. This effect did not saturate, and a linear fit of the data revealed that the slope of this relationship was 10-fold greater for TFD-etomidate than for etomidate (see legend Figure 3). *S*- and *R*-TFD-etomidate (9 μM) activated

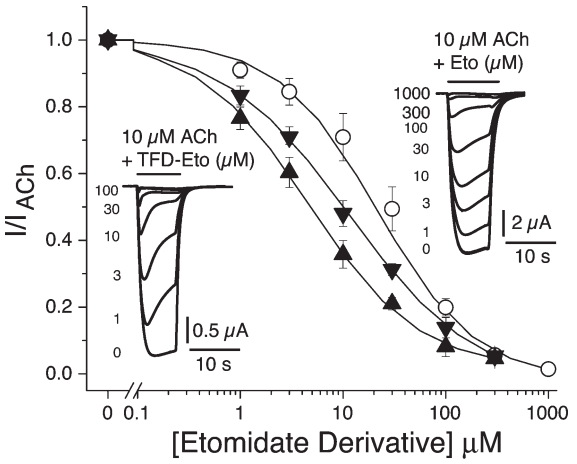

Figure 4. TFD-etomidate is a more potent inhibitor of ACh-induced currents than etomidate. Oocytes expressing wild type *Torpedo* nAChRs were tested with 10 μM ACh ($\sim EC_{10}$) and then with 10 μM ACh plus increasing amounts of etomidate or derivatives. The current traces in the top right inset show one oocyte's current response to 10 μM ACh plus increasing amounts of *R*-etomidate (0, 3, 10, 30, 100, and 300 μM and 1 and 3 mM). The effect of TFD-etomidate on 10 μM ACh currents is shown in the bottom left inset (0, 3, 10, 30, 100, and 300 μM TFD-etomidate). Nonlinear least-squares analysis of the curves yielded: for *R*-etomidate (○), IC_{50} = 21 ± 3 μM, n_H = 0.9 ± 0.1 (3 oocytes); for TFD-etomidate, IC_{50} = 4.1 ± 0.5 μM, n_H = 1.1 ± 0.07 (data not shown, 1 oocyte, each response was tested at least three times at each TFD-etomidate concentration); for *R*-TFD-etomidate (▼), IC_{50} = 11.3 ± 1.6 μM, n_H = 0.7 ± 0.1, and for *S*-TFD-etomidate (▲): IC_{50} = 4.7 ± 0.5 μM, n_H = 0.8 ± 0.1). Currents were normalized to the 10 μM ACh response. Graphs for *R*- and *S*-TFD-etomidate represent data from 2 oocytes with at least 2−3 recordings at each drug concentration.

equally (0.4%), but the effect is small compared to the errors and so we cannot rule out enantioselectivity.

5-HT$_{3A}$ Receptor Antagonist Binding. TFD-etomidate (6.25−70 μM) and etomidate (20−300 μM) caused no consistent changes in displaceable [^{3}H]GR65630 binding (data not shown). Control [^{3}H]GR65630 binding was 33 ± 0.85 pmol/mg. Pooled data revealed no significant changes in [^{3}H]GR65630 binding (unpaired *t* test, $p > 0.01$).

Action on nACh Receptor. When TFD-etomidate was coapplied with acetylcholine to voltage clamped oocytes expressing *Torpedo* nAChR receptors, it inhibited acetylcholine-induced currents (Figure 4). Peak currents elicited by 10 μM ACh (acetylcholine has $EC_{50} \approx 25$ μM for *Torpedo*) were inhibited by increasing amounts of TFD-etomidate with an IC_{50} value of 4.1 ± 0.5 μM. Etomidate behaved similarly but was less potent, having an IC_{50} of 21 ± 3 μM. Surprisingly, the R and S enantiomers of TFD-etomidate inhibited 10 μM ACh-induced currents in an enantioselective fashion; *R*- and *S*-TFD-etomidate had IC_{50}'s of 11.3 ± 1.6 and 4.7 ± 0.5 μM, respectively (Figure 4). TFD-etomidate in the range from 10 to 100 μM showed no direct activation in the absence of acetylcholine of either mouse muscle or *Torpedo* nAChRs (data not shown).

Photoincorporation of [^{3}H]TFD-etomidate into the *Torpedo* nAChR. Photoincorporation of [^{3}H]TFD-etomidate into *Torpedo* nAChR-rich membranes was evaluated by SDS−PAGE followed by fluorography (Figure 5A) or by liquid scintillation counting of excised gel bands (Figure 5B). In the *Torpedo* membrane preparation, nAChRs comprise about 10−20% of the protein, and other prominent polypeptides include rapsyn, a 43 kDa protein that associates with the

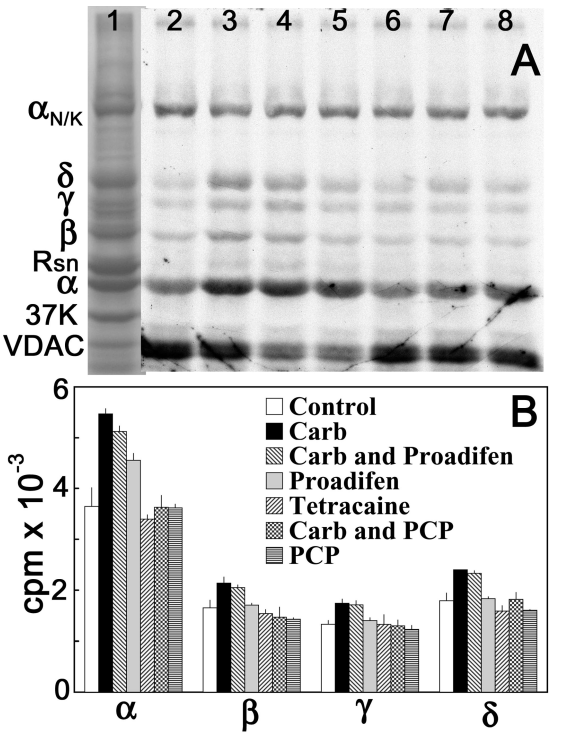

Figure 5. Photoincorporation of [^{3}H]TFD-etomidate into *Torpedo* nAChR. nAChR-rich membranes were photolabeled with 0.3 μM [^{3}H]TFD-etomidate as described in Experimental Procedures. (A) Polypeptides were resolved by SDS−PAGE, visualized by Coomassie Blue Stain (lane 1), and processed for fluorography (14 day exposure, lanes 2−8). Membrane suspensions were photolabeled with [^{3}H]TFD-etomidate in the absence (lane 2) or the presence of 200 μM carbamylcholine (lane 3), 200 μM carbamylcholine and 100 μM proadifen (lane 4), 100 μM proadifen (lane 5), 100 μM tetracaine (lane 6), 200 μM carbamylcholine and 100 μM PCP (lane 7), or 100 μM PCP (lane 8). The stained polypeptide bands corresponding to the nAChR α, β, γ, and δ subunits, rapsyn (Rsn), the α subunit of the Na^+/K^+-ATPase (αN/K, 90 kDa), calelectrin (37K) and the mitochondrial voltage-dependent anion channel (VDAC) are indicated on the left. (B) The ^{3}H incorporation in the excised nAChR α, β, γ, and δ subunit gel bands was determined by liquid scintillation counting (average and range for two photolabelings performed in parallel).

cytoplasmic aspect of the nAChR, calelectrin, a 37 kDa cytoplasmic protein that associates with membranes in a Ca^{2+}-dependent manner, and polypeptides from contaminating membranes from the noninnervated surface of the electrocyte (90 kDa α subunit of the Na^+/K^+-ATPase) and from mitochondria (34 kDa voltage-dependent anion channel (VDAC)).[22]

For membranes photolabeled with [^{3}H]TFD-etomidate in the absence of other drugs, there was ^{3}H incorporation into each of the nAChR subunits, with labeling of the nAChR α subunit most prominent, along with labeling of VDAC and the Na^+/K^+-ATPase α subunit. For membranes labeled in the presence of the agonist carbamylcholine, labeling in the nAChR α subunit was increased by ∼50%, and labeling of the β, γ, and δ subunits increased by ∼30%. To determine whether nAChR subunit labeling was inhibited by drugs known to bind within the nAChR ion channel, membranes were also photolabeled with [^{3}H]TDF-etomidate in the presence of tetracaine, which binds selectively in the ion channel in the closed state, or with proadifen or phencyclidine, drugs that bind in the ion channel with highest affinity when the nAChR is in the desensitized state (i.e., equilibrated with

agonist). The carbamylcholine-enhanced labeling in each nAChR subunit was inhibited by phencyclidine, but not by proadifen. For membranes photolabeled in the absence of agonist, tetracaine did not affect the level of nAChR subunit photolabeling. Proadifen reduced ^{3}H incorporation into VDAC, as had been seen previously for nAChR-rich membranes photolabeled by [^{3}H]azietomidate.[23]

Discussion

General Anesthetic Properties. TFD-etomidate was a reversible general anesthetic in tadpoles and was approximately equipotent to the parent general anesthetic, etomidate. However, *S*-TFD-etomidate was 3.5-fold more potent than *R*-TFD-etomidate, whereas *R*-etomidate is 11-fold more potent than *S*-etomidate.[2,5] Remarkably, inserting the trifluoromethyl diazirinyl group in etomidate's benzene ring reversed the enantioselectivity while having little effect on potency. Godefroi et al (1965) reported several active etomidate derivatives bearing para substituents in the aryl ring, but none with as large a substituent as used herein.

Addition of the trifluoromethyl diazirinyl group increased the octanol−water partition coefficient by 35-fold over that of etomidate, but less than 2-fold over that of TDBzl-etomidate, which bears a substitution in the ester moiety.[6] The potency of a general anesthetic can be predicted with fair accuracy by the empirical Meyer−Overton rule, which states that the product of the anesthetic EC_{50} and the octanol/water partition coefficient is constant. Figure 6 shows such a correlation for 20 agents (see legend) whose potencies cover almost 7 orders of magnitude. Of the enantiomeric pairs of etomidate derivatives, the potencies of *R*-TFD-etomidate, *S*-etomidate and *S*-azietomidate are relatively well predicted by the Meyer−Overton rule. However, all the R-enantiomers of the ester derivatives of etomidate are more potent than predicted, suggesting a favorable specific interaction.[5,24] However, with TFD-etomidate the trend is reversed. The more active enantiomer lies closer to the line, suggesting that the least active enantiomer experiences an unfavorable interaction with its target.

Actions on Ligand-Gated Ion Channels at Anesthetic Concentrations. The puzzling reversal of the enantioselectivity for general anesthesia noted above is partially explained by the action on $GABA_A$Rs. Briefly, *S*- but not *R*-TFD-etomidate enhanced responses to submaximal GABA concentrations. In contrast, both *R*- and *S*-etomidate cause a large enhancement of GABA-induced ion currents, with the S-enantiomer being less potent and slightly less efficacious.[5] However, at the excitatory 5-HT_{3A}Rs and nAChRs, where etomidate has little action at clinical concentrations, TFD-etomidate inhibits in the clinical concentration range. Thus, at twice the LoRR EC_{50}, a concentration corresponding to clinical anesthesia, TFD-etomidate causes an ~1.2-fold left-shift in the GABA concentration−response curve compared to an 18-fold left-shift for etomidate. In contrast, TFD-etomidate causes 33% inhibition of 5-HT_{3A}R currents and *S*- and *R*-TFD-etomidate cause 62% and 30% inhibition of nAChR currents respectively, whereas the equivalent numbers for *R*-etomidate for 5-HT_{3A}R and nAChRs are 4 and 25%, respectively.

Actions on $GABA_A$Rs. *S*-TFD-etomidate's action on GABA-induced ion currents in $\alpha1\beta2\gamma2$L $GABA_A$Rs (Figure 1A) were modest compared to etomidate's.[5] In membranes from cerebral cortex, which would contain $GABA_A$R with a wider range of subunit compositions, TFD-etomidate did not have any allosteric actions on agonist binding (Figure 2A,B).

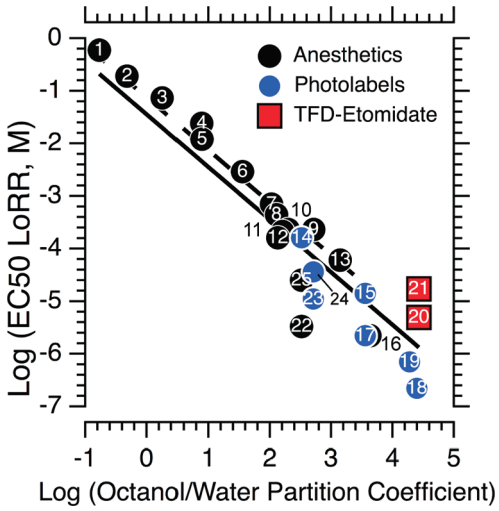

Figure 6. Does the Meyer−Overton rule correctly predict TFD-etomidate's anesthetic potency? The EC_{50} concentration for loss of righting reflexes (LoRR) in tadpoles is plotted against the octanol/water partition coefficient for 25 general anesthetics. The conventional general anesthetics are shown as black circles, and the photoactivable general anesthetics are shown as blue circles except for *R*- and *S*-TFD-etomidate, which are shown as red squares. The solid line is the least-squares fit to all 25 general anesthetics and the dotted line to agents 1−13. The slope was constrained to be −1 as demanded by the Meyer−Overton rule, and the intercepts (± standard deviation) are 1.42 ± 0.12 and −1.13 ± 0.07, respectively. Key #, agent: 1, methanol; 2, ethanol; 3, propanol; 4, diethylether; 5, butanol; 6, pentanol; 7, hexanol; 8, amobarbital; 9, heptanol; 10, halothane; 11, methoxyflurane; 12, pentobarbital; 13, octanol; 14, 3-azioctanol; 15, *S*-(−)-azietomidate; 16, propofol; 17, *R*-(+)-azietomidate; 18, BzBzl-etomidate; 19, TDBzl-etomidate; 20, *S*-TFD-etomidate; 21, *R*-TFD-etomidate; 22, *R*-(+)-etomidate; 23, *R*-(+)-etomidate azide; 24, *S*-(−)-etomidate azide; 25, *S*-(−)-etomidate. Data from refs 5, 6, 20, 24, 38, and 39.

To test whether TFD-etomidate binds to the etomidate site but has low efficacy or whether it acts at a different site, independent of etomidate, we first examined the ability of TFD-etomidate to enhance currents elicited by low GABA concentrations in the presence and absence of a fixed concentration of etomidate. We found that the concentration-dependence of enhancement of GABA currents by TFD-etomidate is unaffected by the presence of a fixed concentration of 1 μM etomidate. Second, we used a $GABA_A$R that contains a methionine to tryptophan mutation on a residue that has been photolabeled by azietomidate.[18] In the $\alpha1\beta2$M-286W$\gamma2$L $GABA_A$R, which is relatively insensitive to etomidate,[21] TFD-etomidate exerted the same action as it did in wild type $\alpha1\beta2\gamma2$L $GABA_A$Rs, whereas azietomidate and TDBzl-etomidate were inactive like etomidate. Both pieces of evidence point to TFD-etomidate having a separate site of action from etomidate and the other photolabels.

Thus, TFD-etomidate occupies a separate site that does not interact allosterically with the etomidate site at the $\alpha-\beta$ subunit interface of the transmembrane domain. This site is also distinct from those for flunitrazepam (at the $\gamma-\alpha$ subunit interface of the N-terminal domain) and muscimol (at the $\beta-\alpha$ subunit interface of the N-terminal domain) and does not interact allosterically with them (Figure 2).

TFD-etomidate's weak actions on $GABA_A$Rs is not shared by TDBzl-etomidate (Table 1), which has a similar

Table 1. Pharmacology of Etomidate and Its Trifluorodiazirine Derivatives

agent	general anesthesia $^{LoRR}EC_{50}$ (μM)	enhancement of EC_{10} GABA currents at twice $^{LoRR}EC_{50}$	enhancement of flunitrazepam binding at $^{LoRR}EC_{50}$	inhibition of 5 HT_3R IC_{50} (μM)	inhibition of AChR IC_{50} (μM)
R-etomidate	2.3[b]	9[b]	120%[c]	60	21[a]
S-etomidate	25[b]	9[b]			
R-TFD-etomidate	17[a]	inhibits[a]	none[a]	9[a]	11[a]
S-TFD-etomidate	4.9[a]	1.8 [a]	none[a]	9[a]	4.7[a]
R-TDBzl-etomidate	0.7[c]	5.4[c]	110%[c]	none (>91)[c]	enhances at ≥ 10 μM[d]

[a] This work. [b] From Husain et al, 2003.[5] [c] From Husain et al, 2006.[6] [d] Nirthanan et al, 2008.[27]

moiety substituted at the ester end of the etomidate backbone, nor by BzBzl-etomidate, with a benzophenone group at the ester position. Both these agents enhance currents robustly. Thus, it is unlikely that the bulky substituent per se is responsible for TFD-etomidate's weak actions. Most likely, the orientation that etomidate adopts in its binding site allows bulky groups to be tolerated at the ester but not the benzoyl end of the drug. Indeed, when iodine was substituted at the para position of the phenyl ring, the IC_{50} of etomidate's inhibition of [^{3}H]ethynylpropylbicycloorthobenzoate ([^{3}H]EBOB) binding to rat cortical membranes in the presence of 1 μM GABA decreased some 20-fold.[40] [^{3}H]-EBOB binds to the resting state of $GABA_A$Rs and ligands that enhance GABA binding therefore decrease its binding. The iodo-substitution also abolished the ability to modulate in the absence of GABA. These data are broadly consistent with the role of trifluoromethyldiazirine substitution reported herein. Such substitutions did not affect binding to 11β-hydroxylase,[19] and it will be interesting to see if TFD-etomidate also binds to this target.

Action on nAChRs and 5-HT_{3A}Rs. In contrast to its weak action on $GABA_A$Rs, TFD-etomidate is the only etomidate derivative that we have studied that inhibits nAChRs and 5-HT_{3A}Rs in the clinical concentration range (see above, and Figures 3 and 4).

Although etomidate derivatives do activate currents in $GABA_A$Rs,[8,25] to our knowledge general anesthetics have not previously been reported to exert this action on a cation-conducting member of the Cys-loop ligand-gated ion channel superfamily. It was thus a surprise to find that TFD-etomidate alone induces 5-HT_{3A}R currents (Figure 3B). This partial agonism was weak. At saturating concentrations, TFD-etomidate only activated $\sim$2% of the maximum current that 5-HT activates. Etomidate also activated currents. Its concentration-dependence was a tenth of, and its efficacy comparable to, that of TFD-etomidate. This effect was not observed in nAChRs. In contrast, etomidate, alone, can elicit GABA currents up to 20%.[5]

More detailed kinetic measurements will be required to understand how TFD-etomidate can activate the 5-HT_{3A}R without inhibiting it. One possibility is that it induces a different open state from the one stabilized by agonist, and that this state has a lower affinity for TFD-etomidate than the regular channel. However, in $GABA_A$Rs anesthetics and agonists are thought to induce a similar open state.[26] In $GABA_A$Rs, the etomidate site that enhances GABA-induced currents is thought to be isosteric with that which activates currents,[8] but it is difficult to see how this would be the case for 5-HT_{3A}Rs. However, we can rule out a mechanism whereby TFD-etomidate binds to the agonist site, because even saturating concentrations do not displace the 5-HT_{3A}R antagonist, GR65630.

One further clue to the location of the site of TFD-etomidate's activation of 5-HT_{3A}Rs above comes from TDBzl-etomidate's action on nAChRs. TDBzl-etomidate, which incorporates the same photoreactive aryl diazirine at the opposite end of the etomidate structure (Scheme 1), causes potentiation of currents elicited at submaximal ACh concentrations (Table 1). In this case, TDBzl-etomidate photoincorporates at two distinct sites. The first is an inhibitory site within the lumen of the ion channel, and the second, a novel site, most likely the enhancing site, is at the interface between the alpha and gamma subunits in the transmembrane domain.[27]

Photoincorporation of TFD-etomidate into nAChRs. [^{3}H]-TFD-etomidate photoincorporated into all nAChR subunits equally in the resting state. Photolabeling was enhanced in the agonist−bound desensitized state, ruling out the agonist-binding site as a site of photolabeling. Photolabeling of the agonist site has previously been observed with azietomidate[23] but not TDBzl-etomidate.[27] The location of the desensitization-enhanced photolabeling is likely in the channel, because phencyclidine, a drug that binds in the ion channel with highest affinity when the nAChR is in the desensitized state, antagonized such labeling.

The pharmacological specificity of [^{3}H]TFD-etomidate labeling at the subunit level differs qualitatively from that seen for [^{3}H]TDBzl-etomidate, for which the most prominent effect was a doubling of α-subunit photolabeling in the presence of PCP that was not seen in the presence of agonist.[27] For [^{3}H]TDBzl-etomidate, the PCP-enhanced photolabeling of the α-subunit resulted from labeling of the novel binding site referred to above in the nAChR transmembrane domain at an interface between subunits. Suggestively, the magnitude of the enhancement of [^{3}H]TFD-etomidate photolabeling is comparable to that seen for [^{3}H]TDBzl-etomidate at its novel binding site, but much more detailed studies will be required to determine if this is so and to delineate the other sites.

Conclusion. TFD-etomidate is a general anesthetic with an unusual pharmacologic profile (Table 1). Although behaviorally it appears to be comparable to etomidate in its general anesthetic action, its actions on the Cys-loop ligand-gated ion channels were often unexpected. Thus, further explorations of its pharmacology may yield novel information.

We designed TFD-etomidate to put the reactive group at the opposite end of etomidate from that in TDBzl-etomidate with the goal of further exploring the binding pocket that azietomidate has revealed in the $\alpha-\beta$ subunit interface of $GABA_A$Rs. Although we obtained some useful structure−activity relationship information about this pocket because the agent appears not to interact with it, our original goal is thereby frustrated. At the same time, this very observation enhances TFD-etomidate's usefulness for exploring other unknown sites of its general anesthetic action, so that in the end it may prove more broadly useful than we expected when devising it for a more focused purpose.

Experimental Section

Materials. Anhydrous dichloromethane, diisopropylcarbodiimide, *p*-(dimethylamino)pyridine, and Merck silica gel 60 A, 230−400 mesh, were obtained from Aldrich (Milwaukee, WI). *R*-(+)-Etomidate was a kind gift from Organon Laboratories (Newhouse, Lancashire, Scotland). *R*-(+)-Etomidate used in $GABA_A$ receptor electrophysiology studies was purchased from Bedford Laboratories (Bedford, OH) as a 2.0 mg/mL solution in 35% propylene glycol/water (v/v). All other chemicals were from Sigma (St. Louis, MO). cDNAs for the α1, β2 and γ2L subunits of human $GABA_A$ receptors in pCDM8 vectors were gifts from Dr. Paul J. Whiting (Merck Sharp & Dohme Research Laboratories, Essex, UK).

Analytical Chemistry. ^{1}H NMR spectra were recorded on a Jeol Eclipse 400 MHz spectrometer in $CDCl_3$ with tetramethylsilane as reference by Acorn NMR Spectroscopy Service (Livermore, CA). UV spectra were recorded on a Hewlett-Packard spectrophotometer. HPLC analysis was performed on a Varian Prostar instrument with a C-18 reversed phase column (Varian, Walnut Creek, CA). Resolution of racemic TFD-etomidate was performed on Chiracel OD-H analytical column using hexane; isopropanol 95/5 and UV detection at 220 nm. Tritiation by esterification with labeled ethanol was performed by American Radiochemical (St. Louis, MO). Mass spectral analyses were performed by AnaSpec, Inc. (San Jose, CA). Elemental analyses were performed by Galbraith Laboratories (Knoxville, TN); all compounds were >95% pure. Optical rotation measurements were performed by Organix Inc. (Woburn, MA) at 20 °C on Jasco P-1010 polarimeter in a 10 cm cell at concentrations expressed as g/100 mL.

(1-(4-Bromophenyl)ethoxy)(*tert*-butyl)dimethylsilane (2). To a solution of 4-bromo-α-methylbenzyl alcohol (18.1 g, 0.09 mol) and *t*-butyl-dimethylsilyl chloride (14.65 g, 0.099 mol) in anhydrous dichloromethane (100 mL) at room temperature under argon was added dropwise a solution of DBU (15.8 g, 15.5 mL, 0.104 mol) in anhydrous dichloromethane (100 mL). After being stirred at room temperature for 1 h, the mixture was extracted successively with water (200 mL), 0.1 M HCl (200 mL), twice with saturated sodium bicarbonate solution (200 mL) and water (200 mL). The organic layer was separated and dried over sodium sulfate. After rotary evaporation, the product was purified by silica gel chromatography with hexane to yield 24.8 g (88% yield) of a colorless, liquid silane derivative **2**. ^{1}H NMR spectrum: ($CDCl_3$) δ 7.41 and 7.20 (4H, AA′/BB′ phenyl), 4.81 (q, 1H, methine), 1.37 (d, 3H, methyl), 0.90 (s, 9H, methyl), 0.01 (d, 6H, methyl). Calcd. for $C_{14}H_{23}BrOSi$: C, 53.33%; H, 7.53%. Found: C, 53:88%; H, 7.22%.

(1-(4-(1-(*tert*-Butyldimethylsilyloxy)ethyl)phenyl)-2,2,2-trifluoroethanone (3). The fluoroketone was synthesized following the procedure described by Fishwick et al.[28] that converts bromo compounds to fluoroketone in high yield. The silyl-protected bromo compound **2** (23.7 g, 75 mmol) in anhydrous THF (200 ml) was cooled to −78 °C in ether/dry ice bath and treated under argon by dropwise addition of *n*-butyl lithium (54.6 mL of 1.6 M solution in hexane) over a period of 1 h. After the solution was stirred at −78 °C for 75 min, a solution of diethyl trifluoroacetamide (16.9 g, 99.4 mmol) in anhydrous THF (50 mL) was added dropwise over a period of 1 h. The mixture was stirred at −78 °C for 75 min. The reaction mixture was quenched by adding 200 mL of saturated ammonium chloride solution without warming. The mixture was brought to room temperature overnight. Ether (400 mL) was added and the mixture extracted twice with water (200 mL). The ether layer was dried over magnesium sulfate. After evaporation, the residue was taken up in hexane and applied to a column of silica gel equilibrated with hexane. Elution with 10% dichloromethane/hexane (10:90) gave 21.5 g (89% yield) of the fluoroketone **3**. ^{1}H NMR spectrum: ($CDCl_3$) δ 8.04 and 7.51 (4H, AA′/BB′ phenyl), 4.94 (q, 1H, methine), 1.41 (d, 3H, methyl), 0.92 (s, 9H, methyl), 0.01 (d, 6H, methyl). Calcd. for $C_{16}H_{23}F_3O_2Si$: C, 57.81%; H, 6.97%. Found: C, 58.09%; H, 7.14%.

(1-(4-(1-(*tert*-Butyl)dimethylsilyloxy)ethyl)phenyl)-2,2,2-trifluoroethanone oxime (4). The fluoroketone was converted to oxime as described by Shih & Bayley.[29] A mixture of the fluoroketone **3** (15.7 g, 48.9 mmol), hydroxylamine hydrochloride (4.1 g, 58.6 mmol), and anhydrous pyridine (25 mL) was heated at 75 °C for 4 h. Ethanol (12 mL) was added and the mixture heated at 60 °C for 2 h. The solvent was removed by rotary evaporation, the residue taken in ether (200 mL) and extracted three times with 200 mL portions of water. After the ethereal layer was dried over magnesium sulfate, the solvent was removed by rotary evaporation and the residue applied to a column of silica gel, equilibrated with hexane/dichloromethane (75:25). Elution with dichloromethane gave the oxime **4**. ^{1}H NMR spectrum: ($CDCl_3$) δ 7.45 and 7.44 (4H, AA′/BB′ phenyl), 4.92 (q, 1H, methine), 1.42 (d, 3H, methyl), 0.92 (s, 9H, methyl), 0.01 (6H, methyl). Calcd. for $C_{16}H_{24}F_3NO_2Si$: C, 55.31%; H, 6.96%; N, 4.03%. Found: C, 55.33%; H, 7.25%; N, 4.16%.

(1-(4-(1-(*tert*-Butyl)dimethylsilyloxy)ethyl)phenyl)-2,2,2-trifluoroethanone *o*-Tosyl Oxime (5). To a stirred, ice-cooled solution of the oxime **4** (11.7 g, 34.8 mmol), triethylamine (4.3 g, 5.9 mL, 42.2 mmol) and dimethyl aminopyridine (3868 mg, 3.7 mmol) in anhydrous dichloromethane (50 mL) were slowly added tosyl chloride (7.6 g, 39,8 mmol). After the addition was complete, the mixture was stirred at room temperature for 30 min, extracted three times with 50 mL portions of water, the organic layer was dried over magnesium sulfate, the solvent was removed by rotary evaporation and the residue was purified on a column of silica gel, equilibrated with 20% dichloromethane in hexane. Elution with 50% dichloromethane in hexane yielded the tosylate **5** (13.7 g, 94%). ^{1}H NMR spectrum: ($CDCl_3$) δ 7.90 (m, 2H, phenyl), 7.40 (m, 6 H, phenyl), 4.90 (q, 1H, methine), 2.48 (s, 3H, methyl), 1.41 (d, 3H, methyl), 0.92 (s, 9H, methyl), 0.01 (6H, methyl). Calcd. for $C_{23}H_{30}F_3NO_4Si$: C, 55.07%; H, 6.03%. Found: C, 54.92%; H, 6.03%.

3-(4-(1-(*tert*-Butyl)dimethylsilyloxy)ethyl)phenyl)-3-((trifluoromethyl)-diaziridine (6). A solution of the tosylate **5** (13.6 g, 30 mmol) in anhydrous ether (8 mL) was added to liquid ammonia (25 mL) at −78 °C and stirred at −45 to −35 °C for 6 h. The solution was slowly allowed to come to room temperature and stirred overnight. The mixture was taken in ether (75 mL), filtered, and the precipitate was washed with ether. Rotary evaporation of the ethereal solution gave 9.36 g of a viscous residue of the diaziridine **6** which was taken to the next step without further purification.

3-(4-(1-(*tert*-Butyl)dimethylsilyloxy)ethyl)phenyl)-3-((trifluoromethyl)-3*H*-diazirine (7). To a mixture of the crude diaziridine **6** (9.36 g, 28 mmol) and triethylamine (5 mL) in dichloromethane (20 mL), cooled in ice, was added solid iodine in small portions until a brownish color persisted (4.3 g iodine required). The mixture was diluted with ether (400 mL) and 10% aqueous citric acid (200 mL). Sodium metabisulfite was added until the color of iodine was discharged. The ethereal layer was separated, washed with water, and dried with magnesium sulfate. The ether was removed by rotary evaporation and the crude product purified on a silica gel column equilibrated with hexane. A faintly pale colored, liquid diazirine **7** (5.51 g, 59%) was obtained. ^{1}H NMR spectrum: ($CDCl_3$) δ 7.35 and 7.13 (4H, AA′/BB′ phenyl), 4.84 (q, 1H, methine), 1.38 (d, 3H, methyl), 0.9 (s, 9H, methyl), 0.01 (6H, methyl). Calcd. for $C_{16}H_{23}F_3N_2OSi$: C, 55.79%; H, 6.73%; N, 8.13%. Found: C, 55.26%; H, 6.79%; N, 8.30%.

3-(4-(1-(Bromoethyl)phenyl)-3-((trifluoromethyl)-3*H*-diazirine (8). The *tert*-butyldimehylsilyl protecting group of the diazirine **7** was replaced by a bromo group by the procedure of Aizpurua et al.[30] A solution of the diazirine **7** (5.5 g, 16.5 mmol) in anhydrous dichloromethane (25 mL) was added to a suspension of triphenylphosphine dibromide (7.7 g, 18.1 mmol) in

anhydrous dichloromethane (40 mL). The mixture was stirred at room temperature for 15 h. The solution was diluted with dichloromethane (125 mL), extracted twice with 100 mL of water, and dried over sodium sulfate. The product was purified on a silica gel column, equilibrated with hexane to yield the bromo compound **8** (4.2 g, 87% yield). Because of its instability, the bromo compound was taken immediately to the next step without further purification.

1-(4-(3-((Trifluoromethyl)-3*H*-diazirin-3-yl)phenyl)ethanamine (9). A solution of the bromo compound **8** (4.1 g, 14 mmol) in methanol (100 mL) was saturated with ammonia and the solution was kept for 72 h in a closed vessel. The solution was rotary evaporated and the residue was taken up in ether (100 mL) and shaken with 1 M NaOH to breakup any hydrochloride. The ether layer was separated, washed with brine, and dried over sodium sulfate. The crude product was purified by chromatography on a column of silica gel, equilibrated with 10% ether in dichloromethane. Elution with the equilibration solvent containing 10% methanol provided a pale colored amine **9** (2.1 g, 65% yield). ^{1}H NMR spectrum: ($CDCl_3$) δ 7.39 and 7.16 (4H, AA′/BB′ phenyl), 4.12 (q, 1H, methine), 1.61 (s, 2H, amino), 1.36 (d, 3H, methyl). Calcd. for $C_{10}H_{10}F_3N_3$: C, 52.40%; H, 4.40%; N, 18.33%. Found: C, 52.03%; H, 4.48%; N, 17.66%.

Ethyl 2-(1-(4-(3-((trifluoromethyl)-3*H*-dazirin-3-yl)phenyl)ethylamino)butanethanoate (10). To a solution of the amine **9** (2 g, 8.9 mmol) and triethylamine (1.23 mL, 8.9 mmol) in anhydrous dimethylformamide (8 mL), cooled in an ice bath, was slowly added ethyl chloroacetate (1.085 g, 948 μL, 8.86 mmol). After the addition was complete, the ice bath was removed and the solution was stirred at room temperature for 48 h. The mixture was diluted with ether (30 mL), filtered, and the precipitate was washed with ether. The ethereal layer was extracted three times with 30 mL portions of ether and dried over magnesium sulfate The crude product was purified on a silica gel column, equilibrated with dichloromethane. Washing with the equilibrium solvent followed by elution with the equilibration solvent containing 10% ether yielded the pale liquid glycine ester derivative **10** (2.26 g, 81% yield). ^{1}H NMR spectrum: ($CDCl_3$) δ 7.36 and 7.2 (4H, AA′/BB′ phenyl), 4.15 (q, 2H, methylene), 3.81 (q, 1H, methine), 3.21 (q, 2H, methylene), 1.35 (d, 3H, methyl), 1.24 (t, 3H, methyl). Calcd. for $C_{14}H_{16}F_3N_3O_2$: C, 53.33%; H, 5.11%; N, 13.33%. Found: C, 52.76%; H, 5.22%; N, 12.72%.

Ethyl 2-(*N*-(1-(4-(3-(trifluoromethyl)-3*H*-diazirin-3-yl)phenyl)ethyl)methanamido)ethanoate (11). Formylation of **10** was performed with formic anhydride by the procedure of Waki & Meienhofer.[31] A solution of 2 M formic acid in dichloromethane (8 mL) was added dropwise with stirring and with cooling by ice bath to a solution of diisopropylcarbodiimide 1.01 g, 8 mmol in anhydrous dichloromethane (10 mL). After being stirred for 5 min, the mixture was added over a period of 30 min to an ice-cooled solution of the glycine ester **10** (1.26 g, 4 mmol) in anhydrous pyridine (10 mL). The solution was stirred at ice-bath temperature for 4 h. After removal of the solvent by rotary evaporation, the residue was suspended in ether and the insoluble residue was removed by centrifugation. The crude product was purified by chromatography on a silica gel column, equilibrated with dichloromethane. Elution with the equilibration solvent, containing 10% ether yielded 1.3 g (95%) of a pale colored, viscous formyl derivative **11**. ^{1}H NMR spectrum showed splitting of signal in a ratio of 0.74:0.26, especially in formyl, methyl, and methylene protons adjacent to the nitrogen atom, indicating the presence of cis−trans isomers in that ratio. ^{1}H NMR: ($CDCl_3$) δ 8.41 and 8.18 (1H, formyl), 7.35 and 7.2 (4H, AA′/BB′ phenyl), 5.81 and 4.87 (q, 1H, methine), 4.10 and 4.05 (q, 2H, methylene), 4.15 (m, 2H, methylene), 1.57 (m, 3H, methyl;), 1.20 (m, 3H, methyl). Calcd. for $C_{15}H_{16}F_3N3O_3$: C, 52.48%; H, 4.70%; N, 12.24%. Found: C, 52.75%; H, 4.77%; N, 11.68%.

2-Mercapto-1-(1−4-(3-((trifluoromethyl)-3*H*-diazirin-3-yl)-phenyl)ethyl)-1*H*-imidazol-5-yl propanoate (12). Ring closure of the formyl compound **11** to mercapto imidazole derivative and subsequent oxidative desulfuration was performed by the procedure of Jones et al.[32] as modified by Godefroi et al.[1] Sodium ethoxide was freshly prepared by adding anhydrous ethanol (181 μL, 3.1 mmol) to 34% paraffinic suspension of sodium (210.4 mg suspension, containing 71.5 mg, 3.1 mmol, sodium) in anhydrous tetrahydrofuran (2 mL) under argon. To this suspension was added at 10 °C ethyl formate (676 μL, 8.4 mmol), followed by the formyl derivative **11** (961 mg, 2.8 mmol). The reaction mixture was stirred at room temperature overnight. The suspension was rotary evaporated, the residue was extracted with a mixture of xylene (9 mL) and water (3 mL), the aqueous layer was separated, and the xylene layer was washed with water. The aqueous layer was acidified with 12.1 M conc. HCl (0.57 mL, 6.85 mmol). Potassium thiocyanate (293 mg) was then added, and the suspension was stirred at room temperature for 48 h. The mixture was extracted with chloroform, the organic layer was separated and rotary evaporated to yield the mercapto derivative **12**, which was oxidatively desulfurized in the next step without further purification.

Ethyl 1-(1-(4-(3-((Trifluoromethyl)-3*H*-diazirin-3-yl)phenyl)-ethyl)-1*H*-imidazole-5-carboxylate (TFD-etomidate, 13). To a stirred solution of sodium nitrite (12.5 mg), concentrated nitric acid (1.06 mL, 14.8 mmol) in water (5 mL), cooled to 10 °C, was slowly added a solution of the thiol compound **12** in chloroform (5 mL). The solution was then stirred at room temperature for 1.5 h. Solid sodium bicarbonate (0.75 mg) was carefully added. The chloroform layer was separated and extracted with brine and the organic layer was dried over magnesium sulfate. Rotary evaporation yielded crude product (585 mg). The product was purified by silica gel chromatography with dichloromethane containing 10% ether to yield white crystalline solid diazirinyl etomidate **13** (360 mg, 36% based on the formyl derivative). TLC, Silica gel: dichloromethane/ether 90:10 v/v, single spot, Rf 0.17. HPLC (Zorbax SB-C18 column, gradient A = 0.1% TFA, B = acetonitrile), 10−100% B in 30 min. One peak, retention time 18 min 38 s. ^{1}H NMR spectrum: ($CDCl_3$) δ 7.78 ((s, 1H, imidazole CH), 7.76 (s, 1H, imidazole CH), 7.26 and 7.14 (4H, AA′/BB′ phenyl), 6.36 (q, 1H, methine), 4.24 (m, 2H, methylene), 1.85 (d, 3H, methyl), 1.30 (t, 3H, methyl). UV spectrum (methanol) λ_{max} 358 nm, ε = 345 M^{-1} cm^{-1}. Calcd. for $C_{16}H_{15}F_3N_4O_2$: C, 54.55%; H, 4.29%; N 15.90%. Found: C, 54.81%; H, 4.43%; N 16.01%. Mass spectral analysis: (ESI +ve) M/Z: calculated for (C16 H15 F3 N4 O2 +H)+ 353, found 353. Judged by HPLC analyses the purity is 99%.

Resolution of racemic TFD-etomidate: chromatography of TFD-etomidate on an analytical Chiracel OD-H column with hexane/isopropanol 95:5 at a flow rate of 0.9 mL/min resolved the racemic mixture into S and R enantiomers that eluted at 12.5 and 15.5 min, respectively.

Synthesis of *R*-and *S*-Enantiomers of TFD-etomidate by Mitsunobu Reaction.

***S*- and *R*-3-(4-(1-(*tert*-Butyl)dimethylsilyloxy)ethyl)phenyl)-3-((trifluoromethyl)-3*H*-diazirine (7).** The S- and R-enantiomers of **7** were synthesized starting with *S*- and *R*-4-bromo-α-methylbenzyl alcohol **1** (Aldrich Chemicals lot certification: $[\alpha]^{20}D$ = −38.2 and +38.8 deg (C = 1%, $CHCl_3$) for the S and R enantiomer, respectively) as described in the earlier section.

***S*- and *R*-1-(4-(3*H*-diazirin-3-yl)-2,2,2-trifluoroethyl)ethanol (14).** The silyl-protected *S*- and *R*-diazirine derivatives **7** were deprotected as follows: To a solution of *S*- or *R*-**7** (2.8 g, 8.13 mmol), in anhydrous THF (8 mL) was added a solution of 1 M tetrabutylammonium fluoride in THF (12 mL) at 0 °C. The resulting solution was stirred at room temperature for 17 h, then 20 mL of a saturated solution of ammonium chloride was added, the THF layer was separated and the aqueous layer was extracted twice with 10 mL portions of ether. The combined organic extracts were washed with saturated NaCl solution and

dried over magnesium sulfate. The crude product was purified by chromatography on silica gel with hexane/dichloromethane (75:25) followed by elution with dichloromethane to yield the *S*-diazirinylalcohol **15** (1.76 g, 94% yield). ^{1}H NMR spectrum: ($CDCl_3$) 7.42 and 7.18 (4H, AA′/BB′ phenyl), 4.92 (m, 1H, methine), 1.82 (hydroxyl), 1.48 (t, 3H, methyl). The optical rotations of (*S*)- and (*R*)-**14** ($[\alpha]^{20}D = -27.3$ and $+28.0$ deg (C = 1%, ethanol) for the *S*- and *R*-enantiomer, respectively) indicated that the diazirinyl alcohol retained the chirality of the starting bromoalcohol **1**.

(*R*)-TFD-etomidate (13). Mitsunobu reaction between ethyl-1*H*-imidazole carboxylate and (*S*)-**14** was carried out as described by Zolle et al. for the synthesis of chiral metomidate.[19] A solution of (*S*)-**14** (253 mg, 1.1 mmol) in anhydrous THF (2 mL) was added dropwise to a stirred solution of ethyl-imidazole carboxylate (154 mg, 1.1 mmol) and triphenylphosphine (345 mg, 1.3 mmol) in anhydrous THF (2 mL) under an atmosphere of argon at −30 °C. A solution of *tert*-butylazodicarboxylate (304 mg, 1.3 mmol) in anhydrous THF (2 mL) was added slowly and the temperature was allowed to increase gradually to 0 °C in 2 h. The mixture was then stirred at room temperature for 18 h. The THF was removed by rotary evaporation, and the residue was taken up in ether (5 mL) and stirred for 4 h. The precipitate was filtered off and washed 3 times with 2 mL portions of ether. The crude product obtained after rotary evaporation was taken up in dichloromethane (4 mL) and applied to a column of silica gel (20 g), equilibrated with dichloromethane. After washing with dichloromethane, the product *R*-TFD-etomidate (195 mg) was eluted with 10% ether. The product was further purified by preparative TLC on an 1 mm thick silica gel plate with ethylacetate/hexane 50/50 to yield *R*-TFD-product (150 mg). ^{1}H NMR spectrum: ($CDCl_3$) δ 7.78 (s, 1H, imidazole CH), 7.76 (s, 1H, imidazole CH), 7.26 and 7.14 (4H, AA′/BB′ phenyl), 6.36 (q, 1H, methine), 4.24 (m, 2H, methylene), 1.85 (d, 3H, methyl), 1.30 (t, 3H, methyl). Rotation measurement $[\alpha]^{20}D = +41.4$ deg (C = 1%, ethanol) indicated that there was a complete reversal of chirality compared to the starting alcohol, confirming the result obtained by Zolle et al.[19] Analytical chromatography on Chiracel OD-H column indicated that there was less than 0.5% racemization.

(*S*)-TFD-etomidate (13). *S*-TFD-etomidate was synthesized by Mitsunobu reaction between ethyl-1*H*-imidazole carboxylate and (*R*)-**14** by a procedure similar to that described for the synthesis of *R*-TFD-etomidate. The NMR spectrum of the product was identical to that obtained with *R*-TFD-etomidate or racemic TFD-etomidate. $[\alpha]^{20}D = +44.0$ deg (C = 0.7%, ethanol).

Synthesis of [^{3}H]TFD-etomidate. Unlabeled TFD-etomidate was heated with a solution of sodium hydroxide in ethanol at 60 °C for 30 min to obtain the de-esterified intermediate. The hydrolyzed derivative was then re-esterified with [^{3}H]ethanol using diisopropylcarbodiimide, dimethylaminopyridine in anhydrous dichloromethane to produce [^{3}H]TFD-etomidate with a specific activity of 40 Ci/mmol.

Solubility and Partition Properties. To determine solubility, TFD-etomidate (5 mg) was stirred in 0.01 M Tris-HCl buffer, pH 7.4 (1 mL) for 24 h. After centrifugation of the suspension, aliquots were removed from the supernatant and analyzed on an HPLC C-18 reverse phase column (Varian, Walnut Creek, CA). The concentration of the probe in solution was calculated from the peak emerging at the calibrated retention time for the probe. To determine octanol/water partition coefficients, TFD-etomidate or etomidate (4 mg) were stirred in a two phase mixture of octanol (0.4 mL) and 0.01 M Tris-HCl buffer, pH 7.4 (2 mL) for 24 h. Aliquots were removed from the separated phases and applied to the HPLC column. Concentrations of the probe in the two phases were calculated from the peaks emerging at the calibrated retention time for the probe.

General Anesthetic Potency. *Xenopus laevis* tadpoles (*Xenopus* One, Dextor, Michigan) in the prelimb-bud stage (1−2 cm in length) were housed in large glass jars filled with Amquel+ (Kordon, div. of Novalek, Inc., Hayward, CA) treated tap water. Stock solutions of the test compound were made in ethanol. With prior approval of the MGH Subcommittee on Research Animal Care, general anesthetic potency was assessed in the tadpoles as follows. Groups of five tadpoles were placed in foil-covered 100 mL beakers containing varying dilutions of the test compound in 2.5 mM Tris HCl at pH 7.4 under low levels of ambient light. The final concentration of ethanol did not exceed 5 mM, a concentration that does not contribute to anesthesia.[33] Every 10 min tadpoles were individually flipped using the hooked end of a fire-polished glass pipet until a stable response was reached (usually up to 40 min). Anesthesia was defined as the point at which the tadpoles could be placed in the supine position, but failed to right themselves after 5 s (loss of righting reflex, LoRR). All animals were placed in a recovery beaker of Amquel+ treated tap water and monitored for 30−60 min for fatality or full recovery. The quantal concentration response curves were analyzed by the method of Waud[34] using an Excel macro kindly provided by N. L. Harrison, A. Jenkins, and S. P. Singh (Weill Medical College of Cornell University).

Electrophysiology of $GABA_A$, *Torpedo* Nicotinic ACh, and 5-HT3A Receptors. With prior approval by the Massachusetts General Hospital Subcommittee on Research Animal Care, oocytes were obtained from adult, female *Xenopus laevis* and prepared using standard methods and as previously described.[35,36] In vitro transcription from linearized cDNA templates and purification of subunit specific cRNAs was carried out using Ambion mMessage Machine RNA kits and spin columns. For $GABA_A$ receptor studies, oocytes were injected with ∼100 ng of total mRNA (α1, β2, γ2L) mixed at a ratio of 1:1:1 transcribed from human GABA receptor subunit cDNAs in pCDNA3.1. β2M286W $GABA_AR$ mRNA was prepared as described previously.[21] For *Torpedo* nAChR ($(\alpha1)_2\beta1\delta1\gamma1$) studies, oocytes were injected with ∼25 ng of total mRNA mixed at a ratio of $2\alpha{:}1\beta{:}1\gamma{:}1\delta$ as previously described.[36] For human $5\text{-}HT_{3A}$ studies, oocytes were injected with ∼50 ng of cRNA.[35]

All two-electrode voltage clamp experiments were done at room temperature, with the oocyte transmembrane potential clamped at −50 mV and with continuous oocyte perfusion with ND96 (100 mM NaCl, 2 mM KCl, 10 mM Hepes, 1 mM EGTA, 1 mM $CaCl_2$, 0.8 mM $MgCl_2$, pH 7.5) at ∼2 mL/min. TFD-etomidate was dissolved in DMSO at a concentration of 10 mM just prior to use. Intravenous grade etomidate at a concentration of 2 mg/mL (8.2 mM) in 35% propylene glycol was obtained from Ben Venue Laboratories (Bedford, OH). A small stock of *S*-etomidate was solubilized at 1 mg/mL in 35% propylene glycol. Stocks were further diluted in ND96 to achieve the desired concentration.

$GABA_A$ and nAChR Dose−Response Studies. All agonist and agonist plus drug applications were 15−20 s in duration; oocytes were washed ∼3 min between each application. Currents were amplified using an Oocyte Clamp OC-725C amplifier (Warner Instrument Corp), digitized using a Digidata 1322A (Axon Instruments, Foster City, CA), and analyzed using Clampex/Clampfit 8.2 (Axon Instruments) and OriginPro 6.1 software. Dose response data were fit by nonlinear least-squares regression to the Hill (logistic) equations of the general form:

$$I_X/I_{\mathrm{GABA,max}} = (I_{X,\mathrm{max}}/I_{\mathrm{GABA,max}})\times(1/(1+(\mathrm{EC}_{50}/[X])^n))$$

where X is the concentration of the activating ligand, $I_{\mathrm{GABA,max}}$ is the maximally evoked current, EC_{50} is the concentration of X eliciting half of its maximal effect, and n is the Hill coefficient of activation. Inhibition experiments were fit with logistic equations of the form:

$$I = 1-([\mathrm{X}]^n/(\mathrm{IC}_{50}{}^n+[\mathrm{X}]^n))$$

$5\text{-}HT_{3A}R$ Concentration−Response Studies. Currents were amplified with a GeneClamp 500B amplifier (Molecular Device,

Inc., Sunnyvale, CA) and signals were acquired using Axon's pClamp 9.0 software. Preceding and following each current recording at a desired 5-HT test concentration, a maximum control current (for normalization) was obtained by perfusing the oocyte with ND96 buffer for 9 s followed by a 15 s exposure to 100 μM 5-HT to obtain a peak response followed by a 5-min recovery period. Test traces were obtained by first perfusing the oocyte with ND96 buffer for 9 s followed by pre-exposing the oocyte to the etomidate derivative for 30 s, coexposure of the etomidate derivative and 100 μM 5-HT for 30 s followed by a recovery period of 5 min. Peaks were measured and test currents recorded as percent of the average of the flanking maximum control currents. Data were analyzed using Igor Pro 4.07 (Wavemetrics Inc., Lake Oswego, OR) and concentration−response data fitted to the Hill Equation:

$$I = I_{max}/[1 + (IC_{50}/[IC_{50}/\text{agonist}])^n]$$

where I is the peak current evoked by the agonist, IC_{50} is the concentration of anesthetic, which inhibits the peak current to half of the control peak current, and n is the Hill coefficient. The time resolution was considered insufficient to analyze inactivation or desensitization.

Allosteric Regulation of the $GABA_A$ Receptor Ligand Binding. Fresh whole bovine brain was placed on ice, and the cortex was rapidly removed, the gray matter was resected, immersed in 0.32 M sucrose, and frozen at −80 °C. The frozen cerebral cortex was thawed and homogenized in 0.32 M sucrose, 10 mM phosphate buffer (pH 7.4). This homogenate was centrifuged (650g, 10 min, 4 °C), and its supernatant was centrifuged again at 150000g for 48 min. The pellet was resuspended in distilled water and recentrifuged at 150000g for 48 min, and this pellet was washed with 10 mM phosphate buffer (pH 7.4) twice, centrifuged, and finally resuspended in 10 mM phosphate buffer (pH 7.4) and stored frozen at −80 °C. Before use, the frozen suspension was thawed, centrifuged, and washed again with 10 mM phosphate buffer (pH 7.4); the pellet was resuspended with assay buffer (10 mM phosphate buffer (pH 7.4), 135 mM KCl, and 1 mM EDTA). Diluted membranes (400 μL) were incubated in a final volume of 0.5 mL for 1 h at 4 °C with [^{3}H]flunitrazepam (1 nM, 85.2 Ci/mmol, PerkinElmer Life Sciences; final protein concentration, 1 mg/mL) or [^{3}H]muscimol (5 nM, 20 Ci/mmol, PerkinElmer Life Sciences; final protein concentration, 0.25 mg/mL). Nonspecific binding was determined by carrying out incubations in the presence of 7.5 μM flurazepam for [^{3}H]flunitrazepam binding and 1 mM GABA for [^{3}H]muscimol binding. The enhancement by etomidate or TFD-etomidate was measured in parallel at various concentrations (0.01, 0.1, 0.3, 1, 3, 10, 30, and 100 μM) in triplicate. Samples were filtered on GF/B glass fiber filters under suction, the filters washed with 3 mL of assay buffer twice, transferred to scintillation vials and subjected to scintillation counting after addition of 2.5 mL of scintillation fluid (Ecolume, ICN).

$5\text{-}HT_{3A}$ Receptor Antagonist Binding. $5\text{-}HT_{3A}R$ rich membranes, expressed in HEK 293 cells, corresponding to 200 pmol of binding sites, were incubated in triplicate for 2 h at room temperature with 0.5 nM [^{3}H]GR65630 (Perkin-Elmer, Waltham, MA) with or without etomidate or TFD-etomidate. Nonspecific binding was determined in the presence of 1 μM quipazine maleate (Sigma-Aldrich, St. Louis, MO). GF/B glass fiber filters (Whatman) were preincubated in 0.5% Poly(ethyleneimine) solution (P3143, Sigma-Aldrich) for an hour. Samples were filtered under a vacuum and washed twice with 7 mL of cold HEPES/EDTA buffer. Filters were dried under a lamp for 1 h, and [^{3}H]GR65630 was determined by scintillation counting in 5 mL of Liquiscint (National Diagnostics, Atlanta, GA).

Photoincorporation of [^{3}H]TFD-etomidate into the nAChR. nAChR-rich membranes, prepared as described in Middleton & Cohen[37] from *Torpedo californica* electric organs (Aquatic Research Consultants, San Pedro, CA), were resuspended at 2 mg protein/mL in *Torpedo* physiological saline (250 mM NaCl, 5 mM KCl, 3 mM $CaCl_2$, 2 mM $MgCl_2$, and 5 mM sodium phosphate, pH 7.0) supplemented with 1 mM oxidized glutathione. Aliquots (75 μL, 150 pmol ACh binding sites) were incubated at room temperature for 40 min with 0.3 μM [^{3}H]TFD-etomidate (40 Ci/mmol) in the absence or presence of other drugs. The samples were then transferred to a 96-well polyvinyl chloride microtiter plate and irradiated on ice with a 365 nm UV lamp (model EN-16, Spectronics Corporation, Westbury, NJ) for 30 min at a distance of less than 2 cm. Electrophoresis sample buffer (12.5 mM Tris-HCL, 2% SDS, 8% sucrose, 1% glycerol, 0.01% bromophenol blue, pH 6.8) was added to the photolabeled samples, and the polypeptides were resolved on 1.5 mm thick, 8% polyacrylamide/0.33% bis-acrylamide gels. Following electrophoresis, the polypeptides were visualized by staining with Coomassie Blue R-250 (0.25% w/v in 45% methanol and 10% acetic acid). [^{3}H]TFD-etomidate photoincorporation into the membrane polypeptides subunits was visualized by fluorography (Amplify, Amersham Biosciences GE Healthcare) with exposure to film (Kodak BIOMAX XAR Film) for 4−6 weeks, and ^{3}H incorporation into individual polypeptide bands excised from the stained gel was quantified by liquid scintillation counting.[37]

Acknowledgment. This research was supported by a grant from the National Institute for General Medical Sciences to K.W.M. (GM 58448) and by the Department of Anesthesia, Critical Care and Pain Medicine, Massachusetts General Hospital. We thank Dr. Niall Hamilton, Organon Laboratories, UK, for a kind gift of *R*-(+)-etomidate.

References

(1) Godefroi, E. F.; Janssen, P. A. J.; Van Der Eycken, C. A. M.; Van Heertum, A. H. M. T.; Niemegeers, C. J. E. DL-1-(1-Arylalkyl)imidazole-5-carboxylate Esters. A Novel Type of Hypnotic Agent. *J. Med. Chem.* **1965**, *8*, 220–223.

(2) Tomlin, S. L.; Jenkins, A.; Lieb, W. R.; Franks, N. P. Stereoselective effects of etomidate optical isomers on gamma-aminobutyric acid type A receptors and animals. *Anesthesiology* **1998**, *88*, 708–717.

(3) Lambert, J. J.; Belelli, D.; Shepard, S.; Muntoni, A.-L.; Pistis, M.; Peters, J. A. The GABA Receptor: An Important Locus for Intravenous Anaesthetic Action. In *Gases in Medicine: Anaesthesia*; Smith, E. B.; Daniels, S., Eds.; Royal Society of Chemistry: Cambridge, 1998; pp 121−137.

(4) Charlesworth, P.; Richards, C. D. Anaesthetic modulation of nicotinic ion channel kinetics in bovine chromaffin cells. *Br. J. Pharmacol.* **1995**, *114*, 909–917.

(5) Husain, S. S.; Ziebell, M. R.; Ruesch, D.; Hong, F.; Arevalo, E.; Kosterlitz, J. A.; Olsen, R. W.; Forman, S. A.; Cohen, J. B.; Miller, K. W. 2-(3-Methyl-3*H*-diaziren-3-yl)ethyl 1-(1-phenylethyl)-1*H*-imidazole-5-carboxylate: a derivative of the stereoselective general anesthetic etomidate for photolabeling ligand-gated ion channels. *J. Med. Chem.* **2003**, *46*, 1257–1265.

(6) Husain, S. S.; Nirthanan, S.; Ruesch, D.; Solt, K.; Cheng, Q.; Li, G. D.; Arevalo, E.; Olsen, R. W.; Raines, D. E.; Forman, S. A.; Cohen, J. B.; Miller, K. W. Synthesis of trifluoromethylaryl diazirine and benzophenone derivatives of etomidate that are potent general anesthetics and effective photolabels for probing sites on ligand-gated ion channels. *J. Med. Chem.* **2006**, *49*, 4818–4825.

(7) Pistis, M.; Belelli, D.; Peters, J. A.; Lambert, J. J. The interaction of general anaesthetics with recombinant $GABA_A$ and glycine receptors expressed in *Xenopus laevis oocytes*: a comparative study. *Br. J. Pharmacol.* **1997**, *122*, 1707–1719.

(8) Rüsch, D.; Zhong, H.; Forman, S. A. Gating allosterism at a single class of etomidate sites on alpha1beta2gamma2L GABA A receptors accounts for both direct activation and agonist modulation. *J. Biol. Chem.* **2004**, *279*, 20982–20992.

(9) Hill-Venning, C.; Belelli, D.; Peters, J. A.; Lambert, J. J. Subunit-dependent interaction of the general anaesthetic etomidate with the gamma-aminobutyric acid type A receptor. *Br. J. Pharmacol.* **1997**, *120*, 749–756.

(10) McGurk, K. A.; Pistis, M.; Belelli, D.; Hope, A. G.; Lambert, J. J. The effect of a transmembrane amino acid on etomidate sensitivity

of an invertebrate GABA receptor. *Br. J. Pharmacol.* **1998**, *124*, 13–20.
(11) Mihic, S. J.; Ye, Q.; Wick, M. J.; Koltchine, V. V.; Krasowski, M. D.; Finn, S. E.; Mascia, M. P.; Valenzuela, C. F.; Hanson, K. K.; Greenblatt, E. P.; Harris, R. A.; Harrison, N. L. Sites of alcohol and volatile anaesthetic action on GABA(A) and glycine receptors. *Nature* **1997**, *389*, 385–389.
(12) Jurd, R.; Arras, M.; Lambert, S.; Drexler, B.; Siegwart, R.; Crestani, F.; Zaugg, M.; Vogt, K. E.; Ledermann, B.; Antkowiak, B.; Rudolph, U. General anesthetic actions in vivo strongly attenuated by a point mutation in the GABA(A) receptor beta3 subunit. *FASEB J.* **2003**, *17*, 250–252.
(13) Reynolds, D. S.; Rosahl, T. W.; Cirone, J.; O'Meara, G. F.; Haythornthwaite, A.; Newman, R. J.; Myers, J.; Sur, C.; Howell, O.; Rutter, A. R.; Atack, J.; Macaulay, A. J.; Hadingham, K. L.; Hutson, P. H.; Belelli, D.; Lambert, J. J.; Dawson, G. R.; McKernan, R.; Whiting, P. J.; Wafford, K. A. Sedation and anesthesia mediated by distinct GABA(A) receptor isoforms. *J. Neurosci.* **2003**, *23*, 8608–8617.
(14) Rudolph, U.; Antkowiak, B. Molecular and neuronal substrates for general anaesthetics. *Nat. Rev. Neurosci.* **2004**, *5*, 709–720.
(15) Desai, R.; Ruesch, D.; Forman, S. A. Gamma-amino butyric acid type A receptor mutations at beta2N265 alter etomidate efficacy while preserving basal and agonist-dependent activity. *Anesthesiology* **2009**, *111*, 774–784.
(16) Bali, M.; Akabas, M. H. Defining the propofol binding site location on the GABAA receptor. *Mol. Pharmacol.* **2004**, *65*, 68–76.
(17) Liao, M.; Sonner, J. M.; Husain, S. S.; Miller, K. W.; Jurd, R.; Rudolph, U.; Eger, E. I., 2nd. R (+) etomidate and the photoactivable R (+) azietomidate have comparable anesthetic activity in wild-type mice and comparably decreased activity in mice with a N265M point mutation in the gamma-aminobutyric acid receptor beta3 subunit. *Anesth. Analg.* **2005**, *101*, 131–135.
(18) Li, G. D.; Chiara, D. C.; Sawyer, G. W.; Husain, S. S.; Olsen, R. W.; Cohen, J. B. Identification of a GABAA receptor anesthetic binding site at subunit interfaces by photolabeling with an etomidate analog. *J. Neurosci.* **2006**, *26*, 11599–11605.
(19) Zolle, I. M.; Berger, M. L.; Hammerschmidt, F.; Hahner, S.; Schirbel, A.; Peric-Simov, B. New selective inhibitors of steroid 11beta-hydroxylation in the adrenal cortex. Synthesis and structure-activity relationship of potent etomidate analogues. *J. Med. Chem.* **2008**, *51*, 2244–2253.
(20) Bright, D. P.; Adham, S. D.; Lemaire, L. C.; Benavides, R.; Gruss, M.; Taylor, G. W.; Smith, E. H.; Franks, N. P. Identification of anesthetic binding sites on human serum albumin using a novel etomidate photolabel. *J. Biol. Chem.* **2007**, *282*, 12038–12047.
(21) Stewart, D.; Desai, R.; Cheng, Q.; Liu, A.; Forman, S. A. Tryptophan mutations at azi-etomidate photo-incorporation sites on alpha1 or beta2 subunits enhance $GABA_A$ receptor gating and reduce etomidate modulation. *Mol. Pharmacol.* **2008**, *74*, 1687–1695.
(22) Blanton, M. P.; Lala, A. K.; Cohen, J. B. Identification and characterization of membrane-associated polypeptides in *Torpedo* nicotinic acetylcholine receptor-rich membranes by hydrophobic photolabeling. *Biochim. Biophys. Acta* **2001**, *1512*, 215–224.
(23) Ziebell, M. R.; Nirthanan, S.; Husain, S. S.; Miller, K. W.; Cohen, J. B. Identification of binding sites in the nicotinic acetylcholine receptor for [^{3}H]azietomidate, a photoactivatable general anesthetic. *J. Biol. Chem.* **2004**, *279*, 17640–17649.
(24) Sandermann, H. Ecotoxicology of narcosis: stereoselectivity and potential target sites. *Chemosphere* **2008**, *72*, 1256–1259.
(25) Belelli, D.; Lambert, J. J.; Peters, J. A.; Wafford, K.; Whiting, P. J. The interaction of the general anesthetic etomidate with the gamma-aminobutyric acid type A receptor is influenced by a single amino acid. *Proc. Natl. Acad. Sci. U.S.A.* **1997**, *94*, 11031–11036.
(26) Rosen, A.; Bali, M.; Horenstein, J.; Akabas, M. H. Channel opening by anesthetics and GABA induces similar changes in the GABAA receptor M2 segment. *Biophys. J.* **2007**, *92*, 3130–3139.
(27) Nirthanan, S.; Garcia, G., 3rd.; Chiara, D. C.; Husain, S. S.; Cohen, J. B. Identification of binding sites in the nicotinic acetylcholine receptor for TDBzl-etomidate, a photoreactive positive allosteric effector. *J. Biol. Chem.* **2008**, *283*, 22051–22062.
(28) Fishwick, C. W. G.; Sanderson, J. M.; Findlay, J. B. C. An efficient route to S-N-(9-fluorenylmethoxycarbonyl)-4′-(1-azi-2,2,2-trifluoroethyl)phenylalanine. *Tetrahedron Lett.* **1994**, *35*, 4611–4614.
(29) Shih, L. B.; Bayley, H. A carbene-yielding amino acid for incorporation into peptide photoaffinity reagents. *Anal. Biochem.* **1985**, *144*, 132–141.
(30) Aizpurua, J. M.; Cossio, F. P.; Palomo, C. Reagents and synthetic methods. 61. Reaction of hindered trialkylsilyl esters and trialkylsilyl ethers with triphenylphosphine dibromide: preparation of carboxylic acid bromides and alkyl bromides under mild neutral conditions. *J. Org. Chem.* **1985**, *51*, 4941–4943.
(31) Waki, M.; Meienhofer, J. Efficient preparation of N-alpha-formylamino acid tert-butyl esters. *J. Org. Chem.* **1977**, *42*, 2019–2020.
(32) Jones, R. G. Studies on imidazoles. II. The Synthesis of 5-imidazolecarboxylates from glycine and substituted glycine esters. *J. Am. Chem. Soc.* **1949**, *71*, 644–647.
(33) Alifimoff, J. K.; Firestone, L. L.; Miller, K. W. Anaesthetic potencies of primary alkanols: implications for the molecular dimensions of the anaesthetic site. *Br. J. Pharmacol.* **1989**, *96*, 9–16.
(34) Waud, D. R. On biological assays involving quantal responses. *J. Pharmacol. Exp. Therapeut.* **1972**, *183*, 577–607.
(35) Solt, K.; Stevens, R. J.; Davies, P. A.; Raines, D. E. General anesthetic-induced channel gating enhancement of 5-hydroxytryptamine type 3 receptors depends on receptor subunit composition. *J. Pharmacol. Exp. Ther.* **2005**, *315*, 771–776.
(36) Sullivan, D. A.; Cohen, J. B. Mapping the agonist binding site of the nicotinic acetylcholine receptor. *J. Biol. Chem.* **2000**, *275*, 12651–12660.
(37) Middleton, R. E.; Cohen, J. B. Mapping of the acetylcholine binding site of the nicotinic acetylcholine receptor: [^{3}H]nicotine as an agonist photoaffinity label. *Biochemistry* **1991**, *30*, 6987–6997.
(38) Firestone, L. L.; Miller, J. C.; Miller, K. W. Tables of physical and pharmacological properties of anesthetics. In *Molecular and Cellular Mechanisms of Anesthetics*; Roth, S. H.; Miller, K. W., Eds.; Plenum: *New York*, 1986; pp 455−470.
(39) Husain, S. S.; Forman, S. A.; Kloczewiak, M. A.; Addona, G. H.; Olsen, R. W.; Pratt, M. B.; Cohen, J. B.; Miller, K. W. Synthesis and properties of 3-(2-hydroxyethyl)-3-*n*-pentyldiazirine, a photoactivable general anesthetic. *J. Med. Chem.* **1999**, *42*, 3300–3307.
(40) Atucha, E.; Hammerschmidt, F.; Zolle, I.; Sieghart, W.; Berger, M. L. Structure−activity relationship of etomidate derivatives at the GABA(A) receptor: Comparison with binding to 11beta-hydroxylase. *Bioorg. Med. Chem. Lett.* **2009**, *19*, 4284–4287.